Characterization of Carbon Nanotubes by TEM and Infrared Spectroscopy

C. Branca,*,† F. Frusteri,‡ V. Magazù,‡ and A. Mangione†

Dipartimento di Fisica and INFM, Università di Messina, P.O. Box 55, S. ta Sperone C. da Papardo, 98166 Messina, Italy, and Istituto CNR-ITAE, via Salita S. Lucia Sopra Contesse 39, I-98126 Messina, Italy

Received: October 24, 2003; In Final Form: January 20, 2004

Single-walled nanotubes (SWNTs) industrially produced and multiwalled nanotubes (MWNTs) we produced by catalysis were investigated by transmission electron microscopy (TEM) and Fourier transform infrared (FTIR) spectroscopy. The observed spectral features, that is the peak position, intensity, and bandwidth, were related to some structural properties of the investigated samples. In such a way, information on the vibrational modes, nanotube diameters, and purity degree of the samples was obtained. The findings of the FTIR investigation are in perfect agreement with the TEM evidence.

Introduction

The discovery of carbon nanotubes (CNTs) by Iijima[1] in 1991 stimulated intensive experimental and theoretical research on these materials, opening the way for their use in intriguing and novel applications in electronics, chemistry, and materials science. There are two main types of carbon nanotubes characterized by the structure of their wall: single-walled nanotubes, consisting of a graphene sheet rolled up into a cylinder of a few nanometers in diameter and several microns in length,[2] and multiwalled nanotubes, consisting in an arrangement of coaxial tubes of graphite sheets ranging in number from two up to about fifty.[1]

Many applications have been proposed for CNTs, such as field emission displays, supercapacitors, ultrahigh strength materials, and nanometer-sized semiconductor devices, probes, and interconnects.[3−10] In particular, the excellent performance of hydrogen adsorption make them promising in such applications as hydrogen-storage materials for fuel-cell-powered electric vehicles.[11,12]

The first measurements of hydrogen adsorption were performed on highly impure carbon single-wall nanotubes by Dillon et al.[13] They concluded that their results would lead to promising developments for hydrogen storage. Later, Liu et al.[14] determined the adsorption of hydrogen on SWNTs having a purity of 50−60% which they had synthesized by a semi-continuous arc discharge technique, and found a storage capacity of 4.2% at room temperature and under modestly high pressure. This experimental work was accomplished by many theoretical studies. Darkrim and Levesque[15,16] were the first to compute hydrogen adsorption in open carbon nanotubes in a wide range of pressure and temperature. They discussed the influence of the single-walled carbon nanotube diameters on the relative arrangement of carbon atoms and hydrogen molecules within an array of parallel single-walled carbon nanotubes and studied the influence on adsorption of the distance between the nearest-neighbor nanotubes.

Notwithstanding that much attention has been devoted to single-walled nanotubes, it has been shown that multiwalled tubes may offer potential as well. Different works have been performed to investigate the hydrogen adsorption and with the aim of improving the storage capacity of MWNTs by doping them. Unfortunately, the obtained results are strongly controversial.[17−20]

The difficulties of elaboration and purification of the sample used for investigations can drastically influence the obtained results. This explains why many efforts have been devoted to developing new methods of production and cleaning processes. SWCNT production methods are complex, dangerous, and expensive. Most methods—chemical vapor deposition, laser ablation, microwave, and high-pressure CO conversion (HiPco)—use a metal catalyst to encourage carbon to grow in nanotube form without capping.[20,21] However, the use of a metal catalyst dramatically increases the pre- and postproduction costs and the impurities content. MWNTs can also be synthesized from an arc discharge technique[1,13,15,16,22] but they are often obtained from catalytic pyrolysis of hydrocarbides.[23]

Notwithstanding the fact that a large amount of research has been dedicated to the understanding of their physical structures, currently, these properties are still being discovered and disputed. What makes it so difficult is that nanotubes have a very broad range of electronic, thermal, and structural properties that change depending on the different kinds of nanotube (defined by its diameter, length, and chirality, or twist).

Various techniques have been used to characterize the morphology, texture, and structure of CNTs. While Raman spectroscopy on carbon nanotubes is a well-established tool for obtaining information about the surface structures of CNTs and their interaction with adsorbate molecules,[24−30] there are very few infrared investigations on SWNTs and on MWNTs above all[26,31−34] due to poor infrared transmittance of CNT samples and to the poor sample quality of raw material produced. As an additional difficulty the IR-active modes lie close to the frequencies of graphite at 868 and 1590 cm^{-1}, and sometimes it may be difficult to distinguish single-walled nanotubes from multiwalled nanotubes, if the presence of graphitic particles cannot be excluded.

The present work is part of a wider research aimed at optimizing a protocol for hydrogen adsorption in carbon nanotubes. As a preliminary step, the structural properties of some CNT samples, produced by catalytic decomposition of methane with CO_2 on bare and alkali-doped Ni/MgO catalysts,

* Corresponding author. Tel: 0039 0906765025. Fax: 0039 090395004. E-mail: fisika@iol.it.
† Università di Messina.
‡ Istituto CNR-ITAE.

10.1021/jp0372183 CCC: $27.50
Published on Web 02/20/2004

TABLE 1: List of Samples along with the Catalysts, Temperatures, and Reaction Times

sample	catalyst	temperature (°C)	reaction time
A	ICI 65−8	650	15h 15′
B	UCI	650	12h 50′
C	Ni−KO_5	650	12h 50′
D	MPF16−N1=Ni−N1	650	13h 11′

have been characterized by Fourier transform infrared spectroscopy measurements and TEM. A comparison with some industrially produced CNT samples has also been performed.

Experimental Section

Sample Preparation. Carbon nanotube samples were obtained during the catalytic reforming process of methane with CO_2 on bare and alkali-doped Ni/MgO catalysts. In fact, depending upon the reaction conditions and catalyst features, the formation of "whisker" and "encapsulating" carbon species can be observed during the hydrocarbons reforming using a catalyst such as Ni.

In particular, it can be observed that the effects of reaction temperature (650−800 °C) and K addition on the process of carbon deposition on Ni/MgO catalyst under methane dry reforming conditions can be at the origin of the different structures of carbon deposition in bare and promoted systems.

With the aim of producing CNT samples, a Ni/MgO catalyst (MPF) was prepared by the incipient wetness method using a 10% (vol/vol) C_2H_5OH−cyclohexane solution of nickel acetylacetonate ($Ni(C_5H_7O_2)_2$), and MgO "smoke powder" and K-doped Ni/MgO catalysts were obtained by "wet impregnation" of the calcined MPF catalyst with isopropyl alcohol solutions of the potassium acetate salt. After K addition (2.5 wt %), the samples were dried overnight at 80 °C and then calcined at 400 °C for 16 h.

All the catalyst samples were pressed (400 bar), crushed, and sieved, and the 40−70 mesh fraction was used for catalytic measurements. The list of samples along with the catalysts, temperatures, and reaction times is reported in Table 1.

At the end of the process it was observed that the filamentous carbon formation at 650 °C involves the destruction of the bare Ni/MgO structure leading to the detachment of the Ni particles from the support; that considerably lower amounts of carbon deposits with a shell-like (encapsulated carbon) morphology were observed at 800 °C, pointed out that the Boundard reaction was the main route of carbon deposition.

Furthermore, the electronic effect induced by K on the active phase of the Ni/MgO system markedly hindered the rate of coking affecting the morphology of the carbon whiskers by inhibiting the process of carbon diffusion across Ni particles.

TEM Measurements. Samples for TEM were prepared by the grinding of the powder and successive ultrasonic treatment in isopropyl alcohol for 1 min. A drop of the suspension was dried on the standard TEM sample grid covered with holey carbon film. CM12 Philips TEM was used for observations. To measure statistical distributions, negatives were scanned with a flatbed Epson scanner equipped with transparency adapter. Image magnification was calibrated once by 0002 lattice fringes of graphite for the negatives obtained at higher magnification and then transferred to lower magnification images by measuring one and the same image feature. Straight pieces of the tubes were used to measure inner and outer diameter; care was taken to measure each filament only once. At these regions, image intensity profiles were measured perpendicular to the tube axis and averaging along the axis was made. Diameter was measured as a distance between mean values of bright/dark contrast oscillations at the edges of the tube walls.

FTIR Measurements. FTIR spectra of the produced CNT samples were collected by a Bomem DA8 Fourier transform infrared spectrometer working with a globar lamp source, a KBr beam splitter, and DTGS/KBr detector. In the employed configuration it has been possible to cover the 400−4000 cm^{-1} range with a resolution of 4 cm^{-1}.

To obtain a good signal-to-noise ratio, 32 repetitive scans were automatically added for each measurement. For all the samples the experimental data were deconvoluted into the minimum number of symmetrical Voigt profiles $V(\omega)$. This distribution, the most suitable for band shape analysis, is a convolution of a Gaussian and a Lorentzian curve

$$V(\omega) = \frac{\int_{-\infty}^{+\infty} \frac{a_0 \exp(-y^2)\,dy}{a_3^2 + \left[\left(\frac{\omega - a_1}{a_2}\right) - y\right]^2}}{\int_{-\infty}^{+\infty} \frac{\exp(-y^2)\,dy}{a_3^2 + y^2}}$$

where a_0 and a_1 are the amplitude and the center of the distribution, respectively, a_2 is a width related to the Gaussian half width at half-maximum, and a_3 is a width depending on the ratio of the Lorentzian half width at half-maximum to a_2.

FTIR measurements have been also carried out on (i) SWNTs produced by Sigma-Aldrich, purity of 50−70% in volume, with an average diameter of 12−15 Å; (ii) SWNTs by CVD process produced by ILJIN Nanotech, purity degree of 30−99% and average diameter of 8 Å. All the spectra were corrected for the baseline. The FTIR spectra of the MWNT samples produced by catalysis were also normalized for the background at 1280 cm^{-1}.

Results and Discussion

TEM Investigations. It is widely accepted that the carbon nanotube diameter can be determined by directly measuring the distance between two dark lines associated with carbon nanotubes in a TEM image. It is well-known, however, that there exist many factors, such as the defocus value and the size of the objective aperture used, that can dramatically change the appearance of the TEM images. Depending on the imaging conditions, both amplitude contrast and phase contrast may be generated by a carbon nanotube in a TEM image. In general the distance between two dark lines is smaller than the real diameter of the nanotubes. The discrepancy between these two values varies with the size of the tube and the alignment of the tube relative to the electron beam, and can be as large as 30% for sub-nanometer carbon nanotubes. For tubes larger than 1.0 nm, the discrepancy is typically less than 10%. The phase contrast of a nanotube changes with the defocus condition.

Representative TEM overviews of the samples investigated are shown in Figure 1. From a qualitative point of view these samples mostly consist of multiwalled nanotubes with a hollow internal channel bearing at the tip, rarely at an intermediate length position, a Ni particle having a size roughly equal to that of the internal diameter of the associated carbon nanotubes. From elemental analysis, no other elements were detected. The samples results show different purity degree and nanotubes concentration. In particular, the samples labeled A and B, that show very similar results, present the higher nanotubes concentration with the larger variety in tube diameters. On the

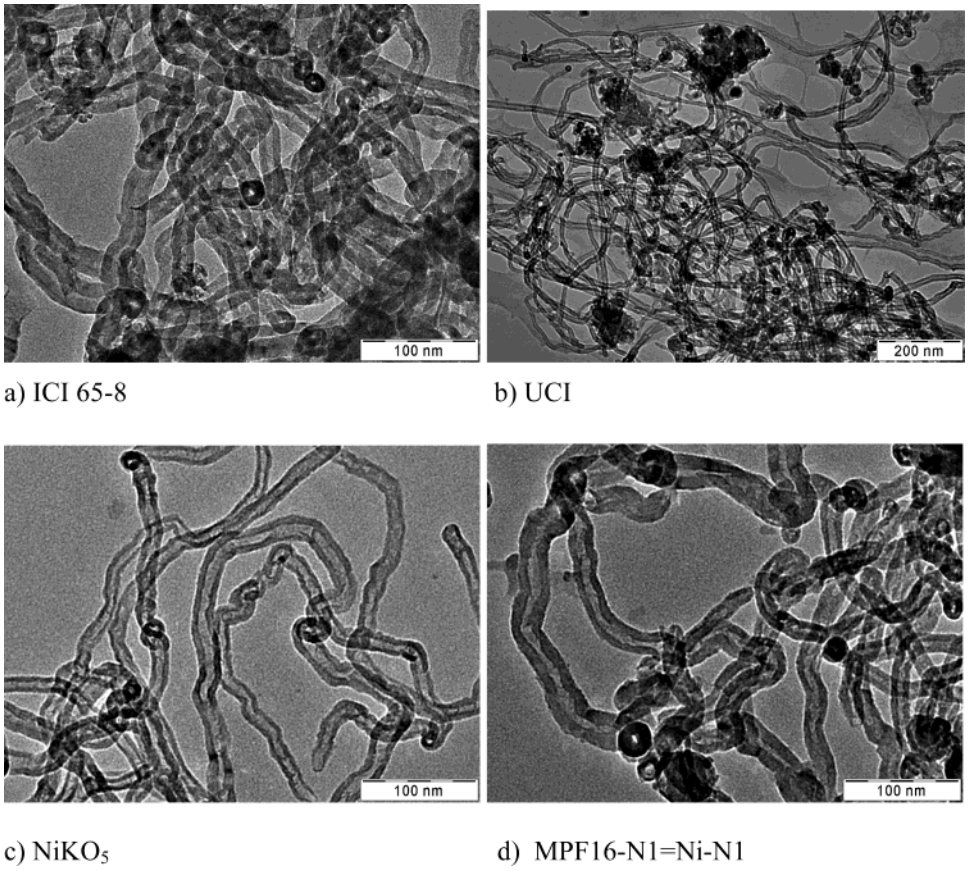

Figure 1. Representative TEM overviews of the carbon samples produced by catalysis.

TABLE 2: Averages of Measurements of the Diameters from Twenty Different TEM Images

sample	d_{int}	d_{ext}
A	76	212
B	76	212
C	70	183
D	66	207

contrary, sample C has the lowest purity degree. Finally, sample D shows an intermediate purity degree. Averages of measurements of the diameters from twenty different images are reported in Table 2.

FTIR Results. In Figure 2 the FTIR spectra of two SWNT samples, one purchased from Sigma-Aldrich and the other from carbon nanotubes-ILJIN, are reported.

As can be seen from Figure 2, in the range between 700 and 2500 cm^{-1} the two SWNT spectra present the same vibrational modes but shifted in energy and with different intensity. In particular, the peaks at 1110 cm^{-1}, 1535 cm^{-1}, and 1700 cm^{-1} observed in the Aldrich sample are shifted to higher wavenumbers in the carbon nanotubes-ILJIN sample by 25 cm^{-1}, 20 cm^{-1}, and 18 cm^{-1}, respectively. Moreover, a very low shoulder is observable in both the spectra between 820 and 840 cm^{-1}. This latter mode, together with the mode around 1540 cm^{-1}, resembles the characteristic modes of graphite at 868 and 1590 cm^{-1}. This is not surprising since, comparing the predictions for IR spectra of SWNTs for different symmetries,[27,35] phonon modes around 850 and 1590 appear in all symmetries almost independently of the diameter and were therefore expected to produce clearly recognizable structures in our infrared spectra.

According to previous works,[36] the number of IR active modes is independent of nanotube diameter. However, the location of the peaks is a sensitive function of the diameter that

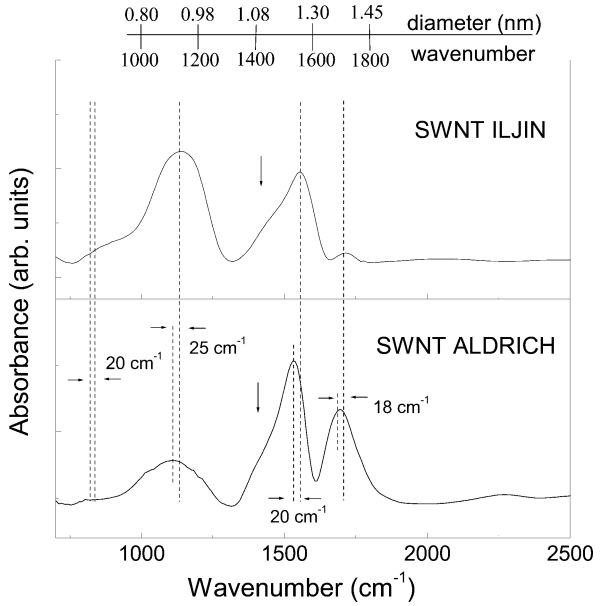

Figure 2. Spectra of SWNT samples produced by Aldrich and by CNT-ILJIN. Spectra have been subtracted for the baseline.

becomes less marked for tubes with a diameter larger than 1.57 nm. In particular, different calculations, proposed to predict the peaks location in SWNTs,[32,37−39] show that smaller diameter tubes exhibit more intense modes at shorter wavenumbers. By using the "adjusted" equation: $d = 8.041 \times 10^{-4}\lambda$, where d is the diameter in nanometers and λ the wavenumber, proposed by Chiang et al.,[32] we can deduce for the Aldrich sample a predominance of tubes with an average diameter of 13 Å; in the ILJIN sample, tubes with a diameter around 9 Å dominate. These findings are in perfect agreement with the product

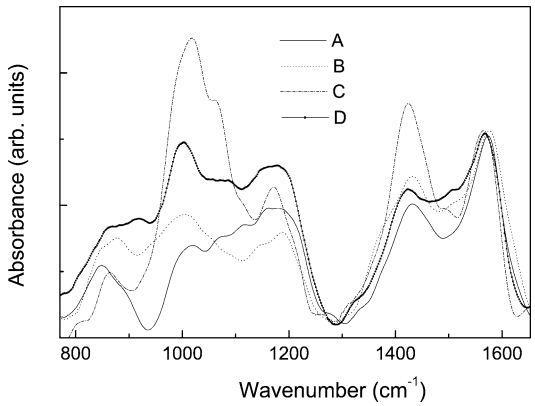

Figure 3. FTIR spectra of the MWNT samples produced by catalysis. Spectra have been subtracted for the baseline and normalized at 1280 cm^{-1}.

specifications furnished by the respective manufacturing home. In Figure 2, a scale bar shows the adjusted tube diameters.

All these considerations suggest to consider not satisfactory the theoretical model based on the force constants[40,41] according by which the upshift to higher frequencies observed in SWNTs should be ascribed to the increasing diameter. According to Kulhmann et al.,[31] this contradiction can be explained taking into account that the force constant models used may lack some detail with respect to the three-dimensional structure of the tubes.

A last consideration can be made on the observed frequency shifts. By taking in mind that, as observed in previous works,[32,33] smaller diameter tubes appear to be preferentially removed by a cleaning process, and the peaks shifted to longer wavenumbers, we can suppose that the cleaning process adopted for the Aldrich sample ensures, on average, a higher purity degree of the sample in comparison with the ILJIN sample. The same conclusion can be drawn by observing the low shoulder present in both spectra around 1430 cm^{-1} (see the vertical arrows in Figure 2). This mode, that can be identified with the Raman mode observed at 1416 cm^{-1} in CNT spectra,[29] may be reasonably assigned to the D-band referred to in the literature which is caused by induction of significant defects or disorder in these nanostructures.[35,42] Starting from these considerations, the comparison between the two spectra allows us to deduce, once more, the presence of a lower content of "defects" in the Aldrich sample in comparison with the ILJIN sample. Also in this case, this consideration is supported by the product specifications.

Let us now direct our attention to the MWNT samples produced by catalysis. Figure 3 presents the FTIR spectra in the energy window between 700 and 1800 cm^{-1}. The spectra have been first subtracted for the baseline and normalized at 1280 cm^{-1}. As can be seen, the spectra show in this range the same vibrational modes centered, within the experimental error, around the same positions but with strongly different intensities and bandwidths. This behavior could be ascribed, especially below 1300 cm^{-1}, to the overlapping of the infrared modes from all the nanotube sizes that are present. TEM evidence seems to justify this interpretation. In fact, the larger distribution of nanotube diameters observed by TEM in samples A and B, in comparison with samples C and D, reflects into a more marked broadening of the IR bands for the A and B samples, whereas the peaks observed for samples C and D are much more well defined. However, to verify this hypothesis, new IR investigations on further purified samples are in progress. In fact, the presence of catalyst components makes difficult the assignment of a well-defined character to the modes present in this region.

In the range between 1300 and 1800 cm^{-1}, two peaks can be observed. The first around 1570 cm^{-1}, together with the broadened peak around 860 cm^{-1}, resembles the graphite modes, whereas the sharp peak at 1430 cm^{-1} is assigned to the D-band. Taking into consideration the origin of this latter contribution just discussed above, we can deduce, in agreement with TEM evidence, the presence of a higher content of defects in the sample C in comparison with the other samples.

Finally, from Figure 3 one can observe that the low wavenumber modes of the sample A and B are strongly suppressed in intensity. Taking in mind the considerations drawn before from the investigations on SWNTs, this observation can be related to the predominance of larger diameter tubes in samples A and B in comparison with samples C and D. Once more, this consideration is supported by TEM evidences.

Conclusions

FTIR spectroscopy was used to characterize industrially produced SWNTs and MWNTs we produced by catalysis. The FTIR investigation revealed the presence in all the spectra of strong structures near the graphite modes but shifted toward lower wavenumbers.

The two SWNT spectra present the same vibrational modes but shifted in energy and with different intensities. The observed spectral features have been related to different nanotube diameters present in the samples. The findings obtained for the SWNTs are in agreement the product specifications furnished by the respective home manufacturing. This testifies to the goodness of the interpretation we adopted and allowed us to perform a structural characterization of the MWNTs we produced by catalysis. In particular, the different intensities observed for the sharp peak at 1430 cm^{-1}, assigned to the D-band and related to the presence of significant defects or disorder in the nanostructures, allowed us to assign a different purity degree to the investigated samples. The obtained findings are in perfect agreement with the TEM evidence.

References and Notes

(1) Jijima, S. *Nature* **1991**, *354*, 56.
(2) Jijima, S.; Ichihashi, T. *Nature* **1993**, *363*, 603.
(3) Baughman, R. H.; Zakhidov, A. A.; de Heer, W. A. *Science* **2002**, *297*, 787.
(4) Lee, N. S.; Chung, D. S.; Han, I. T.; Kang, J. H.; Choi, Y. S.; Kim, H. Y.; Park, S. H.; Jin, Y. W.; Yi, W. K.; Yun, M. J.; Jung, J. E.; Lee, C. J.; You, J. H.; Jo, S. H.; Lee, C. G.; Kim, J. M. *Diamond Relat. Mater.* **2001**, *10*, 265.
(5) An, K. H.; Kim, W. S.; Park, Y. S.; Moon, J. M.; Bae, D. J.; Lim, S. C.; Lee, Y. S.; Lee, Y. H. *Adv. Functional Mater.* **2001**, *11*, 387.
(6) Niu, C. M.; Sichel, E. K.; Hoch, R.; Moy, D.; Tennent, H. *Appl. Phys. Lett.* **1997**, *70*, 1480.
(7) Issi, J. P.; Langer, L.; Heremans, J.; Olk, C. H. *Carbon* **1995**, *33*, 941.
(8) Cornwell, C. F.; Wille, L. T. *Solid State Commun.* **1997**, *101*, 555.
(9) Fuhrer, M. S.; Nygard, J.; Shih, L.; Forero, M.; Yoon, Y. G.; Mazzoni, M. S. C.; Choi, H. J.; Ihm, J.; Louie, S. G.; Zettl, A.; McEuen, P. L. *Science* **2000**, *288*, 494.
(10) Rosen, R.; Simendinger, W.; Debbault, C.; Shimoda, H.; Fleming, L.; Stoner, B.; Zhou, O. *Appl. Phys. Lett.* **2000**, *76*, 1668.
(11) Darkrim, F. L.; Malbrunot, P.; Tartaglia, G. P. *Int. J. Hydrogen Energy* **2002**, *27*, 193.
(12) Froudakis, G. E. *J. Phys. Condens. Mater.* **2002**, *14*, R453.
(13) Dillon, A. C.; Jones, K. M.; Bekkedahl, T. A.; Kiang, C. H.; Bethune, D. S.; Heben, M. J. *Nature* **1997**, *386*, 377.
(14) Liu, C.; Fan, Y. Y.; Liu, M.; Cong, H. T.; Cheng, H. M.; Dresselhaus, M. S. *Science* **1999**, *286*, 1127.
(15) Darkrim, F. L.; Levesque, D. *J. Chem. Phys.* **1998**, *109*, 4981.
(16) Darkrim, F.; Levesque, D. *J. Phys. Chem. B* **2000**, *104*, 6773.
(17) Chen, P.; Wu, X.; Lin, J.; Tan, K. L. *Science* **1999**, *285*, 91.
(18) Yang, R. T. *Carbon* **2000**, *38*, 623.
(19) Tibbetts, G. G.; Meisner, G. P.; Olk, C. H. *Carbon* **2001**, *39*, 2291.

(20) Ding, R. G.; Lu, G. Q.; Yan, Z. F.; Wilson, M. A. *J. Nanosci. Nanotechnol.* **2001**, *1*, 7.
(21) Rinzler, A. G.; Liu, J.; Dai, H.; Nikolaev, P.; Huffman, C. B.; Rodriguez-Macias, F. J.; Boul, P. J.; Lu, A. H.; Heymann, D.; Colbert, D. T.; Lee, R. S.; Fischer, J. E.; Rao, A. M.; Eklund, P. C.; Smalley, R. E. *Appl. Phys. A—Mater.* **1998**, *67*, 29.
(22) Ebbesen, T. W.; Ajayan, P. M. *Nature* **1992**, *358*, 220.
(23) Colbert, D. T.; Zhang, J.; McClure, S. M.; Nikolaev, P.; Chen, Z.; Hafner, J. H.; Owens, D. W.; Kotula, P. G.; Carter, C. B.; Weaver, J. H.; Rinzler, A. G.; Smalley, R. E. *Science* **1994**, *266*, 1218.
(24) Hiura, H.; Ebbesen, T. W.; Tanigaki, K.; Takahashi, H. *Chem. Phys. Lett.* **1993**, *202*, 509.
(25) Chandrabhas, N.; Sood, A. K.; Sundarraraman, D.; Raju, S.; Raghunathan, V. S.; Rao, G. V. N.; Sastry, V. S.; Radhakrishnan, T. S. R.; Hariharan, Y.; Bharathi, A.; Sundar, C. S. *Pramana-J. Phys.* **1994**, 42, 375.
(26) Kastner, J.; Pichler, T.; Kuzmany, H. *Chem. Phys. Lett.* **1994**, *221*, 53.
(27) Dresselhaus, M. S.; Dresselhaus, G.; Eklund, P. C. *Science of Fullerenes and Carbon Nanotubes*; Academic Press: New York, 1996.
(28) Ando, Y.; Zhao, X.; Shimoyama, H.; Sakai, G.; Kaneto, K. *J. Inorg. Mater.* **1999**, *1*, 77.
(29) Zhang, H. B.; Lin, G. D.; Zhou, Z. H.; Dong, X.; Chen, T. *Carbon* **2002**, *40*, 2429.
(30) Ando, Y.; Zhao, X.; Shimoyama, H. *Carbon* **2001**, *39*, 569.
(31) Kuhlmann, U.; Jantoljak, H.; Pfander, N.; Bernier, P.; Journet, C.; Thomsen, C. *Chem. Phys. Lett.* **1998**, *294*, 237.
(32) Chiang, I. W.; Brinson, B. E.; Smalley, R. E.; Margrave, J. L.; Hauge, R. H. *J. Phys. Chem. B* **2001**, *105*, 1157.
(33) Chiang, I. W.; Brinson, B. E.; Huang, A. Y.; Willis, P. A.; Bronikowski, M. J.; Margrave, J. L.; Smalley, R. E.; Hauge, R. H. *J. Phys. Chem. B* **2001**, *105*, 8297.
(34) Liu, L.; Qin, Y.; Guo, Z. X.; Zhu, D. *Carbon* **2003**, *41*, 331.
(35) Eklund, P. C.; Holden, J. M.; Jishi, R. A. *Carbon* **1995**, *33*, 959.
(36) Harris, P. J. F. Carbon nanotubes and related structures. New materials for the twenty-first century; Cambridge University Press: New York, 1999; pp 141−147.
(37) Wildoer, J. W. G.; Venema, L. C.; Rinzler, A. G.; Smalley, R. E.; Dekker, C. *Nature* **1998**, *391*, 59.
(38) Wirth, I.; Eisebitt, S.; Kann, G.; Eberhardt, W. *Phys. Rev. B* **2000**, *61*, 5719.
(39) Odom, T. W.; Huang, J. L.; Kim, P.; Lieber, C. M. *Nature* **1998**, *391*, 62.
(40) Jishi, R. A.; Venkataraman, L.; Dresselhaus, M. S.; Dresselhaus, G. *Chem. Phys. Lett.* **1999**, *209*, 77.
(41) Jishi, R. A.; Venkataraman, L.; Dresselhaus, M. S.; Dresselhaus, G. *Phys. Rev. B* **1995**, *51*, 11176.
(42) Nemanich, R. J.; Solin, S. A. *Phys. Rev. B* **1979**, *20*, 392.